Materials Science-Poland, Vol. 22, No. 4, 2004

Spin-dependent transport and inter-wall coupling in carbon nanotubes

C. J. LAMBERT, S. ATHANASOPOULOS, I. M. GRACE*, S. W. BAILEY

Department of Physics, Lancaster University, Lancaster LA1 4YW, United Kingdom

Theoretical results for electron transport through two structures involving carbon nanotubes are presented. The first structure was a nanotube inserted into another nanotube of a larger diameter. The electrical conductance of the resulting double-wall CNT is an oscillatory function of the length of the insertion. The frequency and amplitude of these oscillations reflect the position dependence of inter-tube interaction in multi-wall CNTs. The second structure was a single-wall carbon nanotube (CNT) in contact with ferromagnetic electrodes, exhibiting giant magnetoresistance (GMR). An intuitive picture of GMR in clean nanotubes with low-resistance contacts is presented and ab initio results are obtained for GMR in Nickel-contacted nanotubes.

Key words: carbon nanotubes; giant magnetoresistance; electron transport

1. Introduction

Multi-wall carbon nanotubes (MWNT) are coaxial cylinders with low translational and rotational energy barriers, which allow the inner tubes to easily slide with respect to the outer tubes [1]. This has been demonstrated by recent experiments, which have shown that it is possible to slide the inner-walls of a MWNT in a "telescope" motion [2, 3], and has led to the suggestion of low-friction, MWNT-based NEMS, such as oscillators with frequencies in excess of 1 GHz [4–6]. One aim of this paper is to demonstrate that the experiments of [2, 3] not only provide a new probe into mechanical inter-wall interactions in MWNTs, but that they also open up the possibility of probing the effect of inter-wall interactions on electronic properties. For single wall nanotubes (SWNTs), electronic properties are primarily determined by chirality [7], whereas in MWNTs the inter-wall interaction can cause the formation of pseudogaps [8] and in the case of telescoping nanotubes, resonances in the differential conductance of ballistic structures [9–11].

*Corresponding author, e-mail: i.grace@lancaster.ac.uk.

Another aim of this paper is to examine spin-polarized transport in CNTs connected to ferromagnetic contacts. Experiments suggesting that CNT-spintronic devices could soon become a reality, including early observations [12] of hysteretic magnetoresistance in Co-contacted nanotubes showed a maximum resistance change of 9%. More recently, Jensen et al. [13] have measured a magnetoresistance ratio of almost 100% in single wall carbon nanotubes contacted with Fe electrodes. In this paper, we investigate Giant Magnetoresistance (GMR) in clean CNTs connected to (n,n) CNT leads coated with Nickel. We compute the change in electrical conductance when the orientation of the magnetization is switched from parallel to antiparallel. The conductance is given by the Landauer formula $G = G_0 Trtt^{\dagger}$, where $G_0 = 2e^2/h$ and t is the transmission matrix.

2. Transport in telescopes and shuttles

We begin with an analysis of the electron transport properties of the telescoping MWNT shown in Fig. 1a, as a function of the displacement δx of the inner tube relative to the outer tube. Using a first principles approach, we predict that transport properties are strongly modified by displacements δx of the order of the interatomic spacing. We also analyse the shuttle structure shown in Fig. 1b, whose electronic properties are closely related to those of the corresponding telescope. Although the mechanical properties of telescoping nanotubes have been investigated experimentally as a function of the length of the telescoping region, no electrical measurements are currently available and the predictions are intended to stimulate such experiments.

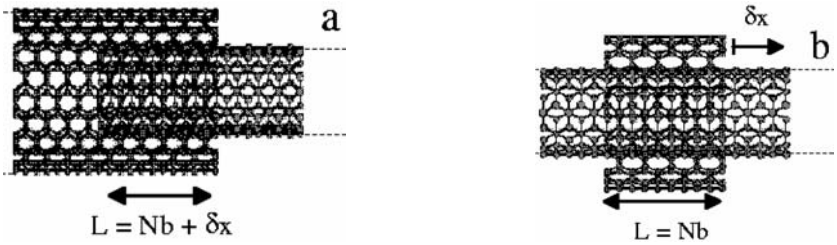

Fig. 1. Telescoping MWNT, in which a small-diameter NT is inserted a distance L into a larger diameter NT (a). The NTs are each connected to reservoirs on the left and right of the structures. In both cases, electrons are scattered at the points, separated by the distance L, where the NTs terminate. A "shuttle" system, in which a large-diameter SWNT (the shuttle) of the length L is placed outside a small-diameter inner wall NT, which in turn is connected to external reservoirs (b)

The problem of computing the δx-dependence of conductance is quite different from the problem considered in [10], where the energy dependence of the electron transmission coefficient is computed for $\delta x = 0$ only. To illustrate this, we note that since a NT is formed by repeatedly joining together identical slices of carbon atoms

(which form the unit cells of the NT), the length L of the overlap region in a telescope can be written as $L = Nb + \delta x$, where b is the length of a slice of the inner or outer NT and δx is a displacement lying between $\pm b/2$ (i.e., $\delta x = L$ modulo b). For an infinite MWNT, the ab initio, mean-field Hamiltonian H is a periodic function of δx, with a period of b, and therefore H must be recomputed self-consistently for each value of δx in order to compute transport properties as a function of displacement.

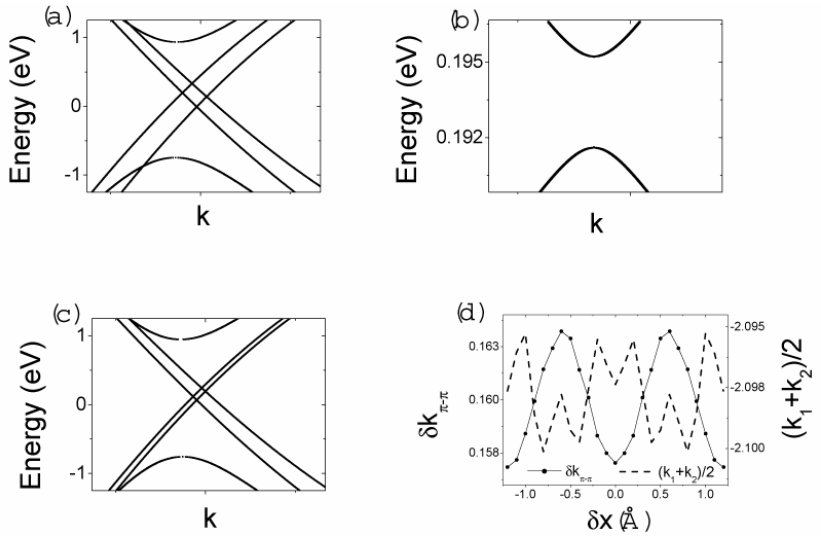

Fig. 2. Ab initio (6,6)@(11,11) band structure close to the Fermi Energy (0 eV) (a). Gap opening due to interwall interaction (b). Band structure with no interwall interaction (c). The difference, $\delta k_{\pi-\pi} = k_2 - k_1$, and average of the π band Fermi wave vectors k_1 and k_2 as a function of δx (d)

The telescope shown in Fig. 1a comprises two coaxial SWNTS, with the inner NT connected to a SWNT extending to $+\infty$ and the outer NT connected to a SWNT with a larger diameter extending to $-\infty$. As a definite example, we focus on the armchair (6,6)@(11,11) MWNT, which has an inter-wall separation of 3.4 Å. This system is typical of most armchair MWNTs, as it does not possess axial symmetry.

In what follows, transport properties are computed using the recursive Greens function scattering technique developed in ref. [14], combined with a Hamiltonian generated using the first principles density functional theory code SIESTA [15]. We use the local density approximation as parameterised by Perdew and Zunger [16] and nonlocal norm-conserving pseudopotentials [18]. The valence electrons are described by a single-ζ basis set. The cut-off radius for the s and p orbitals is chosen to be 4.1 a.u. Before computing transport properties, it is useful to examine the band structure of an infinite (6,6)@(11,11) MWNT. Since the Hamiltonian and overlap matrix elements depend on the positions of the carbon atoms of the inner NT relative to those on the outer NT, this band structure depends on the displacement δx of the inner NT

relative to the outer NT. Figures 2a and b show the calculated band structure of an infinite, non-displaced (6,6)@(11,11) MWNT, corresponding to $\delta x = 0$.

Figure 2a shows that for positive k, in the vicinity of the Fermi energy, the band structure of an infinite MWNT possesses two π bands with positive slope and two π^* bands with negative slope. Several features of this band structure are relevant to understanding transport in telescopes and shuttles. First, as shown in Fig. 2b, in the vicinity of the Fermi energy, small energy gaps of the order of 2meV open at the band crossings. In what follows, we demonstrate that oscillations in transport properties arise over a wide energy range and therefore these gaps are unimportant at most energies. Secondly, the π^* bands of the inner NT are shifted relative to those of the outer NT, mainly due to charge transfer between the NTs. This feature is demonstrated in Fig. 2c, which shows the band structure when all matrix elements between orbitals on the outer and inner NT are artificially set to zero. In this case, the π bands are almost coincident, whereas the π^* bands on the different tubes remain shifted relative to each other. Finally, the π band of the inner NT is shifted relative to that of the outer NT, mainly due to the inter-wall interaction. This is demonstrated by the fact that the main effect of switching on the inter-wall matrix elements (i.e., in going from Fig. 2c to Fig. 2a) is a shift in the π bands, whilst leaving the others almost unaffected. The latter feature is crucial, since it produces large π-π scattering in telescopes and shuttles, while scattering involving other channels remains negligible. In view of the linearity of the bands near E_F, the wave vector difference $\delta k_{\pi\text{-}\pi} = k_2 - k_1$ between the two π

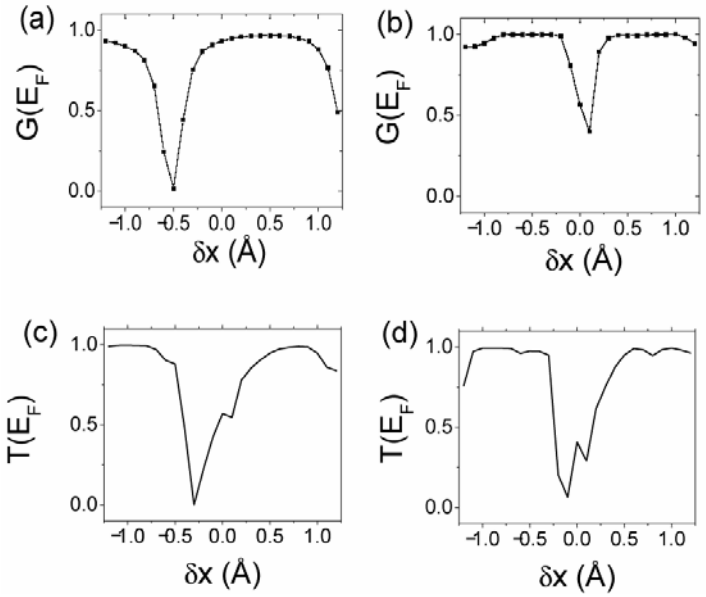

Fig. 3. Ab initio conductance $G(E_F)$ as a function of δx in a (6,6)@(11,11) telescope, for scattering regions of the length: a) $N = 10$, b) $N = 250$. Analytic description of $T(E)$ for the telescope model, for the lengths: c) $N = 10$ and d) $N = 250$

bands is almost independent of energy. The Fermi wave vectors k_1 and k_2 of the π bands, however, are extremely sensitive to the displacement δx of the inner tube relative to the outer tube. This is illustrated in Fig. 2d, which shows the dependence of $\delta k_{\pi\text{-}\pi}$ and $(k_1 + k_2)/2$ on δx. For an infinite MWNT, these quantities are periodic functions of δx, with a period equal to the repeat distance b = 2.45Å of the MWNT.

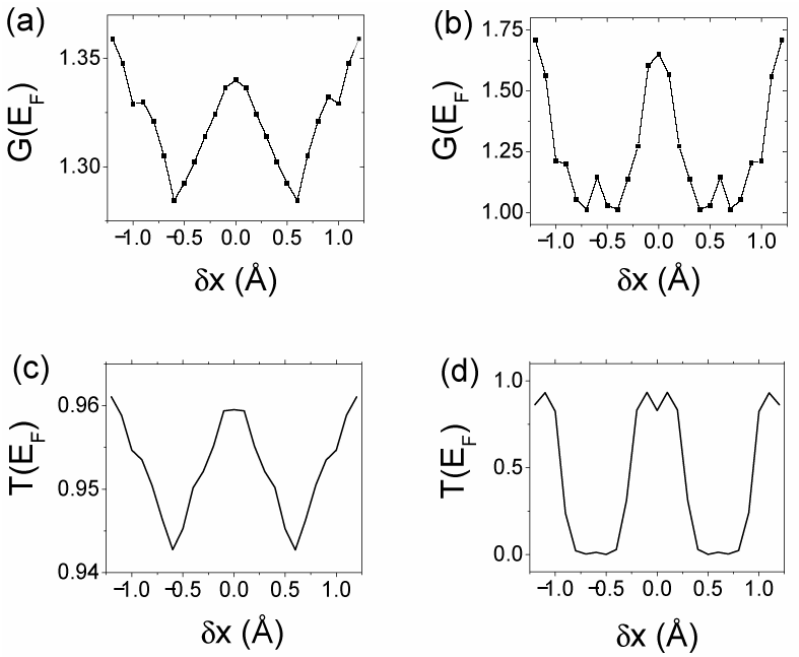

Fig. 4. Ab initio conductance of the shuttle (6,6)@(11,11) nanotube as a function of δx, for scattering lengths: a) N = 10, b) N = 250. Analytic description of transmission for the shuttle model, for the lengths: c) N = 10 and d) N = 250

Having examined the band structure as a function of displacement δx, we now turn to the transport properties of the telescoping (6,6)@(11,11) double wall nanotube and demonstrate that the above δx-dependence of the π wave vectors is accessible via conductance measurements on telescopes and shuttles. For scattering regions of the length $L = Nb + \delta x$, Figs. 3a and b (4a and b) show ab initio results for the electrical conductance $G(E_F) = T(E_F)$ in units of $2e^2/h$ as a function of δx, for a telescope (shuttle) with two values of the number of overlapping slices N. Perhaps the most striking feature of these results is the presence of large oscillations for $\delta x < b$. To demonstrate that these unexpected oscillations are a direct consequence of the δx-dependence of the Hamiltonian, we have developed [19] an analytical description of these oscillations based on retaining only the π-π inter-wall coupling. This approximation is partly justified by comparing Figs. 2a and 2c, which shows that switching on the inter-wall

coupling yields a large shift in the π bands, while leaving the other bands almost unchanged.

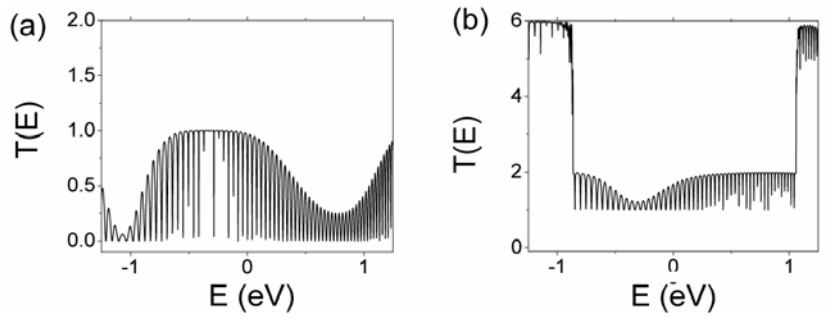

Fig. 5. Transmission coefficient versus energy for a telescope (a) and shuttle (b)

A restriction to π-π coupling is further suggested by comparing the energy dependence of the transmission coefficient for shuttles and telescopes. For $\delta x = 0$, Fig. 5 shows the electron transmission coefficient $T(E)$ versus energy for fixed values of N. For energies in the approximate range ±1 eV, where only the π and π^* scattering channels are open, the transmission coefficient of the telescope (shuttle) oscillates between 0 and 1 (1 and 2). For higher energies, where four additional scattering channels are open, both exhibit remarkably different behaviours. Namely, $T(E)$ for the telescope continues to oscillate between 0 and 1, whereas $T(E)$ for the shuttle increases by 4 and oscillates between 5 and 6. This difference reflects the fact that for the telescope only the π band of the outer tube scatters into the π band of the inner tube and no other channels are transmitted, whereas for the shuttle only the π band of the inner tube is scattered by the presence of the shuttle, while all other channels are transmitted with a probability of almost one. For comparison, Figs. 3c, d, 4c, and 4d show results for this π-π analytical description, the details of which are given in [19].

3. Giant magnetoresistance (GMR) in single-wall CNTs

Using the above first principles approach, we now examine spin-polarised transport in single-wall NTs contacted to ferromagnetic electrodes. Before presenting the exact results, it is useful to have a simple picture of the origin of GMR. Consider the case of armchair (n,n) CNTs, which are metallic with a finite conductance $2G_0$ at the Fermi energy. For an infinitely long CNT with uniform magnetization, the differential conductance of the up-spin carriers, $G_{++}^{\uparrow}$, is shifted by the exchange energy h, and for the down-spin carriers, $G_{++}^{\downarrow}$, by $-h$. The total conductance of the system is $G_{++} = G_{++}^{\uparrow} + G_{++}^{\downarrow}$. In the case of two semi-infinite leads with antiparallel alignment of magnetization, a crude approximation for

the conductance G_{+-} is $G_{+-} = \min 2\left\{G_{++}^{\uparrow}, G_{++}^{\downarrow}\right\}$. As shown in Fig. 6, this simple picture predicts that the difference $G_{++} - G_{+-}$ is non zero only near step edges, where the change in conductance is $\Delta G = (G_{++} - G_{+-})/G_0 = 2$. A similar argument can be applied to zig-zag CNTs.

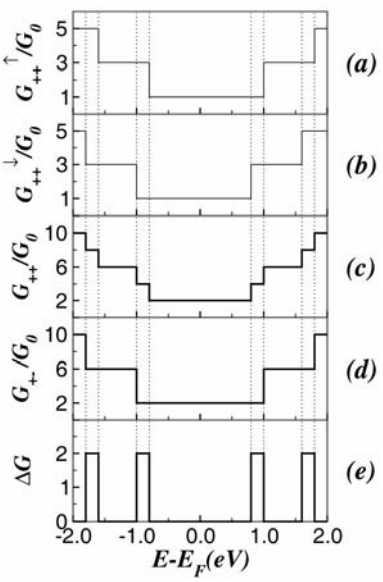

Fig. 6. Differential conductance for the: a) up and b) down spin carriers, total conductance for: c) ferromagnetic and d) antiferromagnetic alignment, and e) relevant change in conductance for metallic armchair CNTs

As a first material-specific calculation of GMR in CNTs, we consider the simplest possible case of a single wall CNT in contact with CNT leads. To induce a magnetic moment in the leads, magnetic Ni impurities are placed along the axis of the leads. For a Ni electrode in contact with a CNT, this situation may occur if Ni atoms migrate along the axis of the CNT. To perform ab initio self-consistent transport calculations, we work within the generalized gradient approximation (GGA) of Perdew–Burke –Ernzerhof [17]. Core electrons are replaced by nonlocal, norm-conserving pseudopotentials (Troulier–Martins) [18], while the valence electrons are described by a linear combination of numerical orbitals. We use a single-zeta basis set for Carbon and a double-zeta singly polarized basis set for Nickel. Real space integrations are performed on a regular grid with an equivalent plane wave mesh cut-off of 150 *Ry*. The atomic positions are relaxed until all force components are smaller than 0.02 eV/Å. After relaxation, the tight binding Hamiltonian for the system can be extracted. Using the recursive Green's function technique [14] we calculate the transmission for a hybrid system consisting of two semi-infinite nanotube leads with Ni atoms located on the CNT axis, in contact with a finite length clean CNT (Fig. 7).

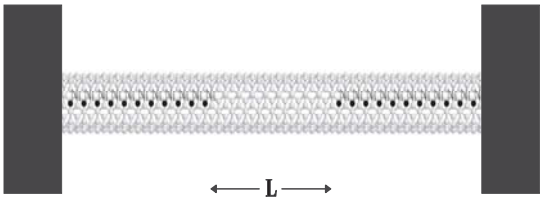

Fig. 7. Armchair carbon nanotube in contact with ferromagnetic electrodes. Ni atoms encapsulated along the axis of a (5,5) CNT

Consider the case of an armchair CNT with Ni atoms located on the axis of the tube, as shown in Fig. 7. Results will be presented for a (5,5) CNT, using a unit cell (i.e., a supercell with a lattice constant a = 2.46 Å) of 20 C atoms and one Ni atom. In the relaxed structure, the Ni atoms remain near their initial positions on the axis of the tube. The total magnetization of the unit cell is $M = 1.71\mu_B$.

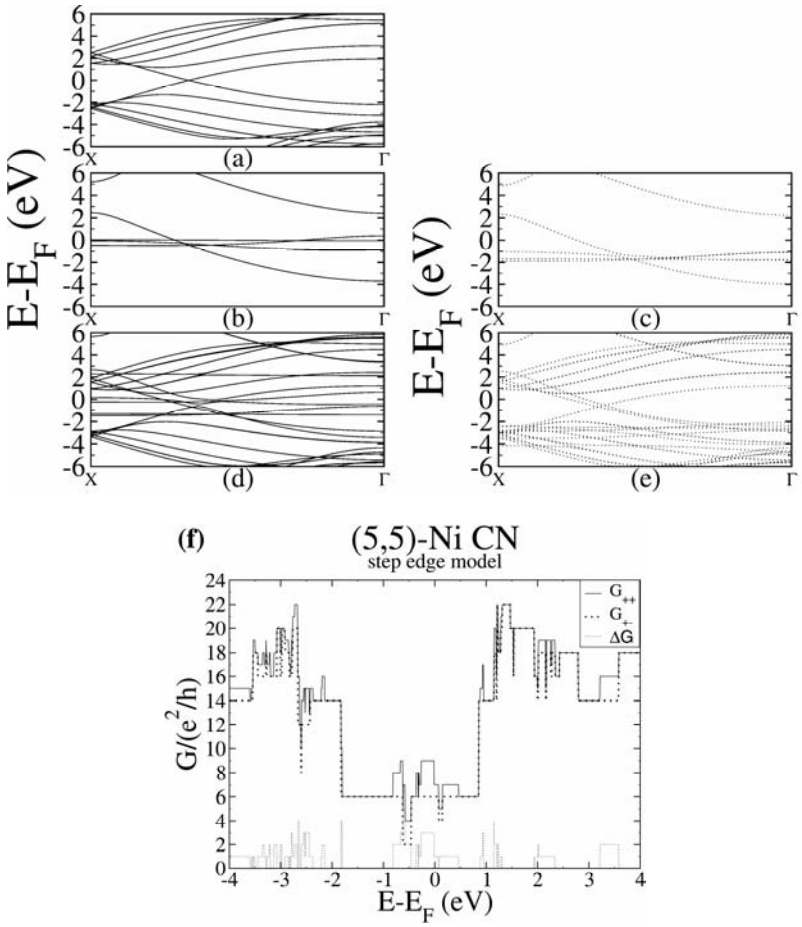

Fig. 8. Band structure for a clean (5,5) CNT (a), the (b) majority and (c) minority spin carriers of a 1-D Ni chain, the (d) majority and (e) minority spin carriers of a (5,5) CNT with coaxial Ni atoms. Step edge model of GMR for a (5,5)-Ni CNT (f)

Figures 8d and e show the band structures for majority and minority spin carriers, respectively. For comparison, Fig. 8a shows the band structure of a clean (5,5) CNT, and Figs. 8b and c the band structures of a 1-D Ni chain for majority and minority spin carriers, respectively. We use a single-zeta basis set for Carbon in the clean (5,5) CNT and a double-zeta singly polarized basis set for Ni in the 1-D chain calculation. The lattice constant for the Ni chain was a = 2.46 Å in order to keep the same interatomic distance between the Ni atoms as in the CNT calculation.

As a prelude to a full transport calculation, we first examine this structure using the above step-edge model of GMR by counting the number of open channels at a specific energy. The resulting step-edge approximation is presented in Fig. 8f, which shows the dimensionless conductances $G_{++}/(e^2/h)$ and $G_{+-}/(e^2/h)$ and the change in conductance $\Delta G = (G_{++} - G_{+-})/(e^2/h)$. To obtain the corresponding ab initio result, we consider two semi-infinite (5,5)-Ni CNT leads, in contact with a clean tube L cells long. For L = 20, the corresponding G_{++} and G_{+-} are shown in Fig. 9a, while the magnetoconductance ΔG is plotted in Fig. 9b. At zero temperature, the GMR ratio $\delta G = \Delta G/G_{++}$ vanishes at the Fermi energy, whereas for nearby energies it takes positive values ≈34%. Fig. 9b also shows that small negative values of GMR occur as well. These are due to multiple scattering from the ends of the CNT and are sensitive to the length L of the scattering region, as discussed in [20].

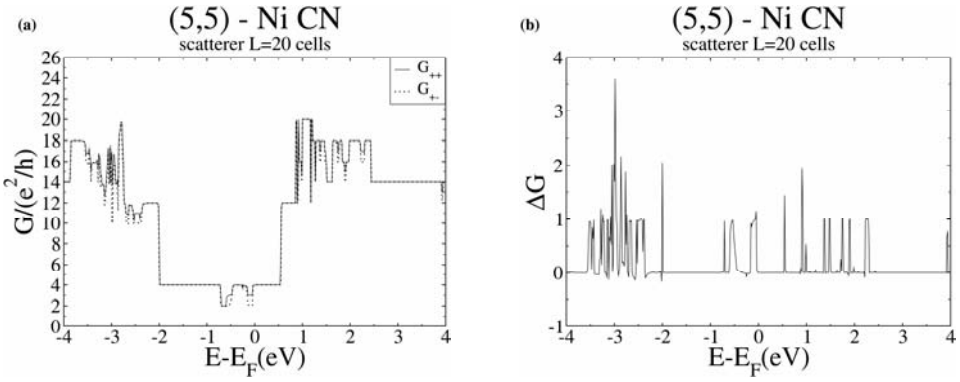

Fig. 9. Differential conductance for ferromagnetic and antiferromagnetic alignment (a) and the relevant change in conductance for a (5,5)-Ni CNT in contact with a clean CNT of the length L = 20 cells

Compared with the step edge model, we find that high values of ΔG are indeed associated with conductance steps in the spin conductances. The ab initio conductances, however, are suppressed compared to the step-edge picture, because the absence of Ni in the scattering region removes a significant number of conducting channels.

4. Conclusions

We have calculated conductance oscillation as a function of the displacement in CNT telescopes and shuttles and argued that these oscillations arise from the depend-

ence on displacement of the coupling between inner and outer tube π channels. The non-monotonic behaviour in the conductance as a function of displacement δx can therefore be used to probe the electronic inter-wall coupling. We have also calculated the magnetoconductance of Ni-contacted CNTs and compared this with a simple step-edge model of GMR. We find that GMR ratios of the order of 34% can be expected in (5,5) armchair CNTs when Ni atoms migrate along the axis of the CNT leads.

Acknowledgements

We are pleased to acknowledge helpful discussions with S. Sanvito and J. Ferrer and support from the EU MCRTN-CT-2003-504574, EPSRC, MoD and the Royal Society.

References

[1] BOURLON B., GLATTLI D.C., BACHTOLD A., FORRO L., http://arxiv.org/abs/cond-mat/0309465 (2003).
[2] CUMMINGS J., ZETTL A., Science 289 (2000), 602.
[3] MIN-FENG YU, YAKOBSON B.I., RUOFF R.S., J. Phys. Chem B, 104 (2000), 8764.
[4] ZHENG Q., JIANG Q., Phys. Rev. Lett., 88 (2003), 45503.
[5] LEGOAS S.B., COLUCI V.R., BRAGA S.F., COURA P.Z., DANTAS S.O., GALVAÕ D.S., Phys. Rev. Lett., 90 (2003), 55504.
[6] RIVERA J.L, MCCABE C.AND CUMMINGS P.T., Nano. Lett., 3 (2003), 1001.
[7] MINTMIRE J.W., DUNLAP B.I., WHITE C.T., Phys. Rev. Lett., 68 (1992), 631.
[8] KWON Y.K., TOMANEK D., Phys. Rev B, 58, R16001 (1998).
[9] SANVITO S., KWON Y.K., TOMANEK D., LAMBERT C.J., Phys.Rev. Lett., 84 (2000), 1974.
[10] KIM D.-H., CHANG K.J., Phys. Rev. B, 66 (2002), 155402.
[11] KIM D.-H., SIM H.-S., CHANG K.J., Phys. Rev. B, 64 (2001), 115409.
[12] TSUKAGOSHI K., ALPHENAAR B.W., AGO H., Nature, 401 (1999), 572.
[13] JENSEN A., NYGARD J., BORGGREEN J., [in:] H. Takayanagi and J. Nitta (Eds.), *Toward the Controllable Quantum States*, Proc. MSS 2002, World Scientific, 2003 , p. 33–37.
[14] SANVITO S., LAMBERT C.J., JEFFERSON J.H., BRATKOVSKY A., Phys. Rev. B, 59 (1999), 11936.
[15] SOLER J.M., ARTACHO E., GALE J.D., GARCÍA A., JUNQUERA J., ORDEJÓN P., SÁNCHEZ-PORTAL D., J. Phys. Condens. Matter., 14 (2002), 2745.
[16] PERDEW J.P., ZUNGER A., Phys. Rev. B (1981), 23, 5048.
[17] PERDEW J.P., BURKE K., ERNZERHOF M., Phys. Rev. Lett., 77 (1996), 3865.
[18] TROULLIER N., MARTINS J.L., Phys. Rev. B, 43 (1991), 1993.
[19] GRACE I.M., BAILEY S.W., LAMBERT C.J., submitted to Phys. Rev. B., 2004.
[20] BABIACZYK W.I., BULKA B.R., http://arxiv.org/abs/cond-mat/0207672 (2002).

Received 15 September 2004
Revised 3 November 2004